

Supporting Information

Design of Carbazole-based Platinum Complexes with Steric Hindrance for Efficient Organic Light-emitting Diodes

Xu-Feng Luo,^a Sheng Ning,^a Hang He,^a Hao Tang,^{a,c} Liang-Jun Shen,^{a,c} Yi-Rui Shen,^{a,c} Hua-Bo Han,^b Xunwen Xiao,^{*a,c} and You-Xuan Zheng,^{*b}

^a*College of Material Science and Chemical Engineering, Ningbo University of Technology, Ningbo 315211, P. R. China.*

E-mail: luoxf@nbut.edu.cn, xunwenxiao@nbut.edu.cn

^b*State Key Laboratory of Coordination Chemistry, School of Chemistry and Chemical Engineering, Nanjing University, Nanjing 210093, P. R. China,*

E-mail: yxzheng@nju.edu.cn

^c*Zhejiang Institute of Tianjin University, 201 Fenghua Road, Ningbo 315201, China*

1. General Descriptions

1.1 Materials and measurements.

All reagents and chemicals were purchased from commercial sources and used without further purification. ^1H and ^{13}C NMR spectra were measured on a Bruker AM 400 spectrometer. Mass spectra (MS) were obtained with ESI-MS (LCQ Fleet, Thermo Fisher Scientific). Absorption and photoluminescence spectra were measured on a UV-3100 spectrophotometer and a Hitachi F-4600 photoluminescence spectrophotometer, respectively. The absolute photoluminescence quantum yields and the decay lifetimes of the compounds were measured with HORIBA FL-3 fluorescence spectrometer. Cyclic voltammetry measurements were conducted on a MPI-A multifunctional electrochemical and chemiluminescent system (Xi'an Remex Analytical Instrument Ltd. Co., China) at room temperature, with a polished Pt plate as the working electrode, platinum thread as the counter electrode and Ag-AgNO₃ (0.1 M) in CH₃CN as the reference electrode, *tetra*-*n*-butylammonium perchlorate (0.1 M) was used as the supporting electrolyte, using Fc⁺/Fc as the internal standard, the scan rate was 0.1 V/s. The single crystal data were obtained by X-ray crystallography measurement with Bruker D8 Venture diffractometer with PHOTON-100 CMOS detector, and then were obtained by absorption correction with SADABS provided by Bruker, and finally refined with olex2 software.

1.2 Theoretical calculation.

The density functional theory (DFT) and time-dependent DFT (TD-DFT) calculations were carried out with Gaussian 09 software package. The geometries of the ground state (S_0) were fully optimized with the B3LYP exchange-correlation functional with lanl2dz basis set for Pt atom and the 6-31G** basis set for the other atoms both in CH₂Cl₂ (C-PCM27 solvent model). Vibrational frequency calculations were performed to validate that they are minima on potential energy surface. On the basis of the optimized S_0 molecular structures in solvent, TD-DFT calculation was performed. Solvent effect was also considered by using C-PCM model. Frontier molecular orbitals were visualized using Gauss View, and their quantified compositions in percentage on different parts were given by QMForge.

1.3 Fabrication and measurements of OLEDs.

Indium-tin-oxide (ITO) coated glass with a sheet resistance of $10 \Omega/\text{sq}$ was used as the anode substrate. Prior to film deposition, patterned ITO substrates were cleaned with detergent, rinsed in de-ionized water, dried in an oven, and finally treated with oxygen plasma for 5 minutes at a pressure of 10 Pa to enhance the surface work function of ITO anode (from 4.7 to 5.1 eV). All the organic layers were deposited with the rate of 0.1 nm/s under high vacuum ($\leq 2 \times 10^{-5}$ Pa). The doped layers were prepared by co-evaporating dopant and host material from two individual sources, and the doping concentrations were modulated by controlling the evaporation rate of dopant. LiF and Al were deposited in another vacuum chamber ($\leq 8.0 \times 10^{-5}$ Pa) with the rates of 0.01, 0.01 and 1 nm s^{-1} , respectively, without being exposed to the atmosphere. The thicknesses of these deposited layers and the evaporation rate of individual materials were monitored in vacuum with quartz crystal monitors. A shadow mask was used to define the cathode and to make ten emitting dots (with the active area of 10 mm^2) on each substrate. Device performances were measured by using a programmable Keithley source measurement unit (Keithley 2400 and Keithley 2000) with a silicon photodiode. The EL spectra were measured with a calibrated Hitachi FL-4600 fluorescence spectrophotometer. The EQE of EL devices were calculated based on the photo energy measured by the photodiode, the EL spectrum, and the current pass through the device.

2. Supplementary data

Table S1. Crystallographic data of *N*-CzPhPtacac and *N*-CzCF₃PhPtacac.

	<i>N</i> -CzPhPtacac	<i>N</i> -CzCF ₃ PhPtacac
Formula	C ₄₀ H ₃₈ N ₂ O ₂ Pt	C ₄₁ H ₃₇ F ₃ N ₂ O ₂ Pt
FW	773.80	843.14
Wavelength (Å)	1.34139	1.34139
Crystal system	monoclinic	monoclinic
Space group	<i>P</i> 21/ <i>c</i>	<i>P</i> 21/ <i>n</i>
<i>a</i> (Å)	12.8788(4)	8.9905(5)
<i>b</i> (Å)	13.2810(4)	13.0648(7)
<i>c</i> (Å)	20.2866(6)	30.8067(16)
α (deg)	90.00	90.00
β (deg)	92.7010(10)	98.192(2)
γ (deg)	90.00	90.00
<i>V</i> (Å ³)	3466.03(18)	3581.6(3)
<i>Z</i>	35	36
ρ_{calcd} (mg/cm ³)	1.483	1.564
μ (Mo K α) (mm ⁻¹)	5.380	5.486
<i>F</i> (000)	1544	1660
Reflns collected	24249	25460
Unique	6313	6357
GOF on <i>F</i> ²	1.044	1.066
<i>R</i> ₁ ^{<i>a</i>} , <i>wR</i> ₂ ^{<i>b</i>} [<i>I</i> > 2 σ (<i>I</i>)]	0.0199, 0.0479	0.0202, 0.0501
<i>R</i> ₁ ^{<i>a</i>} , <i>wR</i> ₂ ^{<i>b</i>} (all data)	0.0224, 0.0493	0.0211, 0.0506

$$R_1^a = \frac{\sum ||F_o| - |F_c||}{\sum F_o}, \quad wR_2^b = [\frac{\sum w(F_o^2 - F_c^2)^2}{\sum w(F_o^2)}]^{1/2}$$

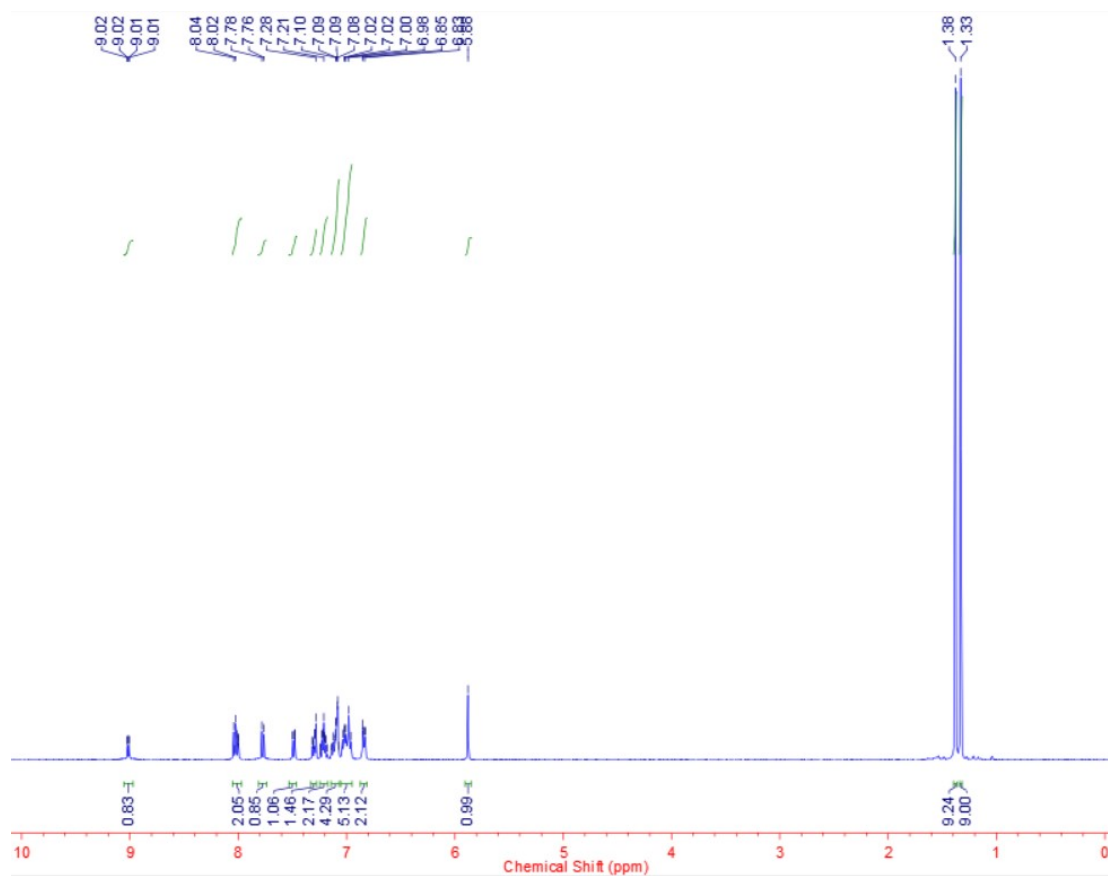


Figure S1. ^1H NMR spectrum of *N*-CzPhPtacac in CDCl_3 .

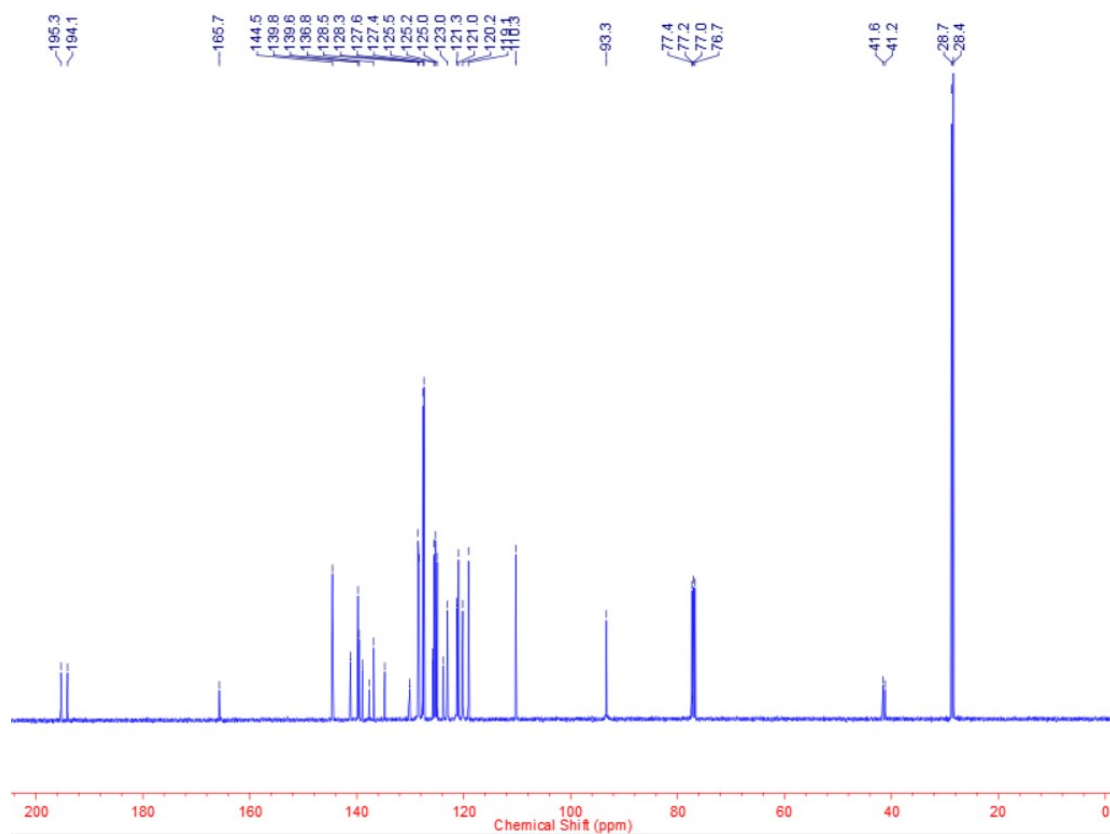


Figure S2. ^{13}C NMR spectrum of *N*-CzPhPtacac in CDCl_3 .

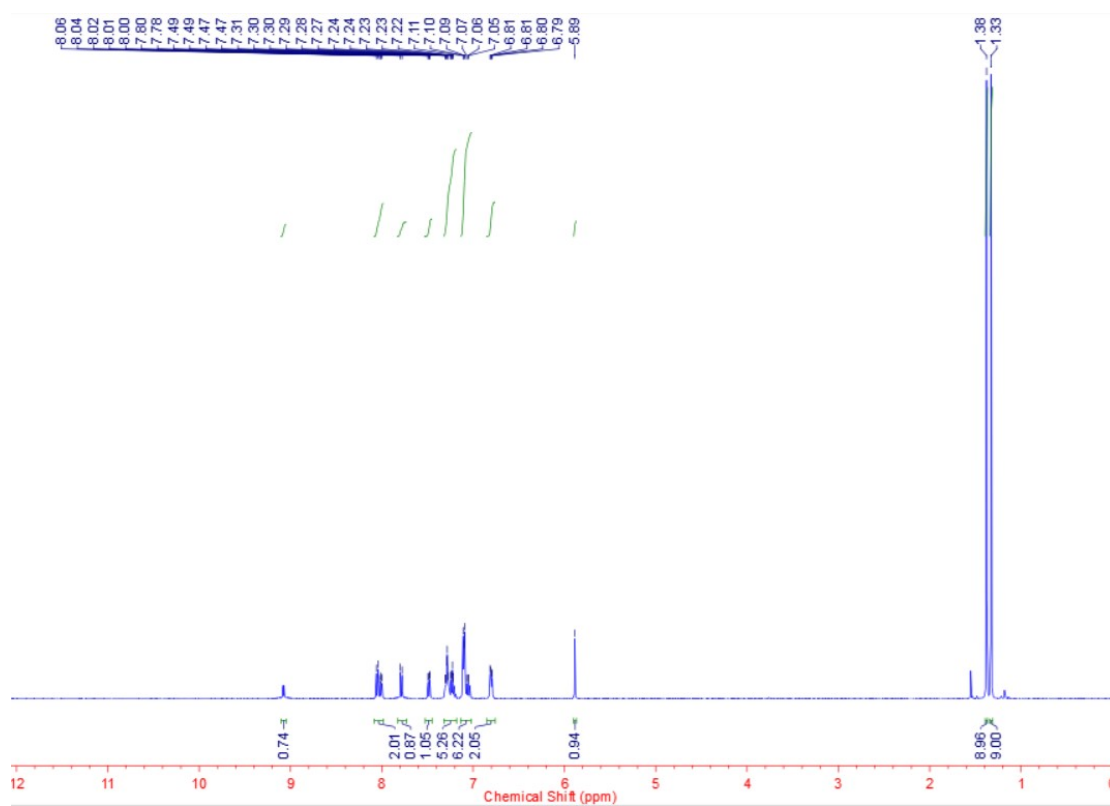


Figure S3. ^1H NMR spectrum of *N*-Cz CF_3 PhPtacac in CDCl_3 .

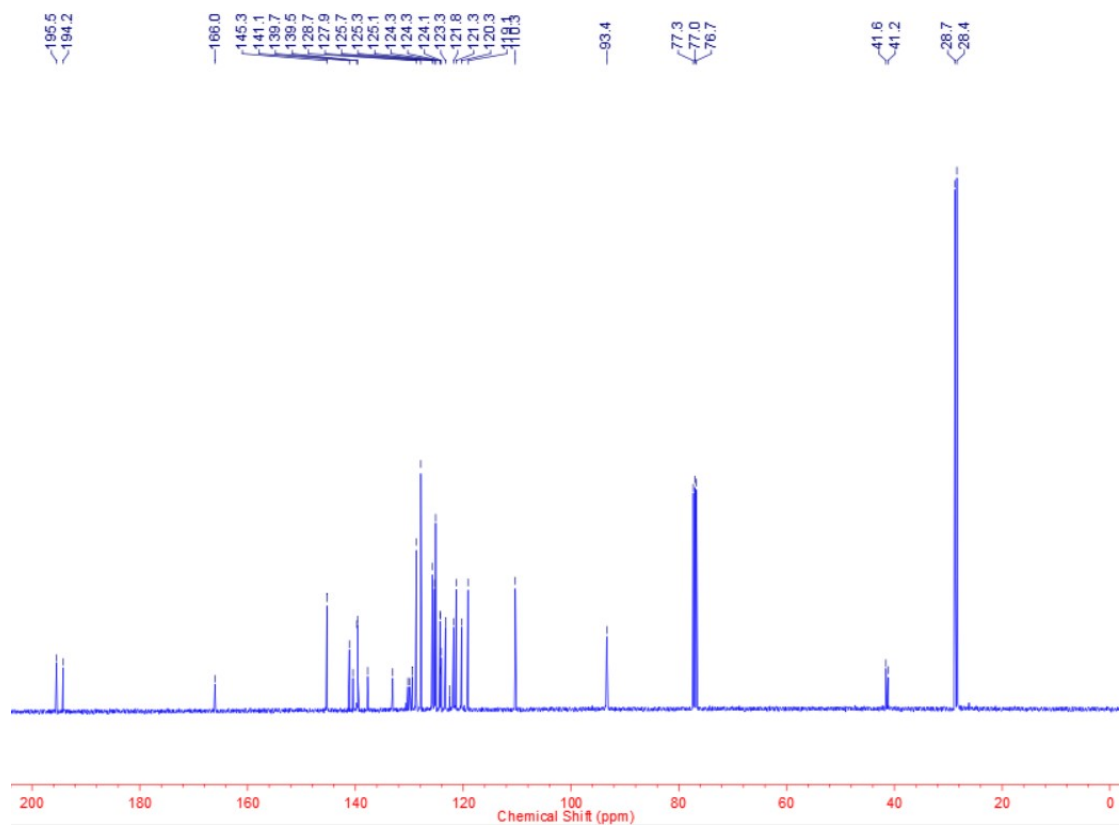


Figure S4. ^{13}C NMR spectrum of $N\text{-CzCF}_3\text{PhPtacac}$ in CDCl_3 .

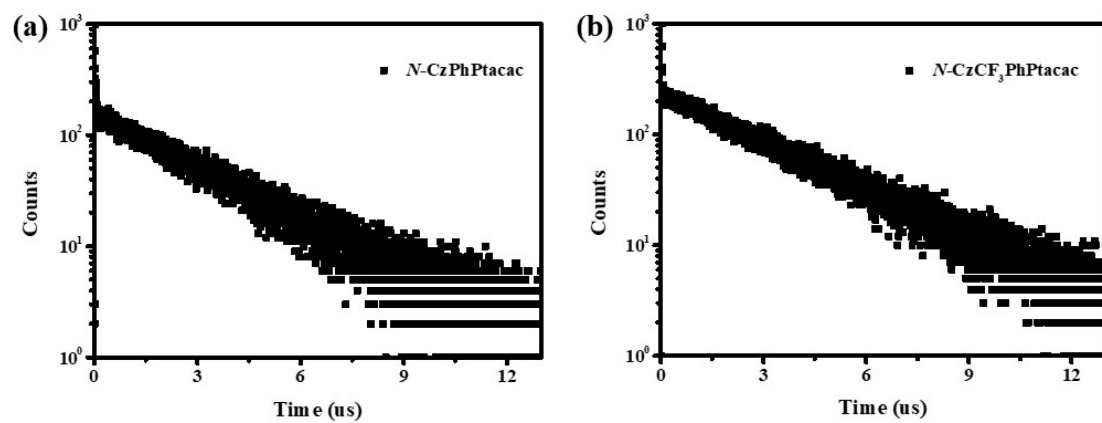


Figure S5. The lifetime curves of both Pt complexes.

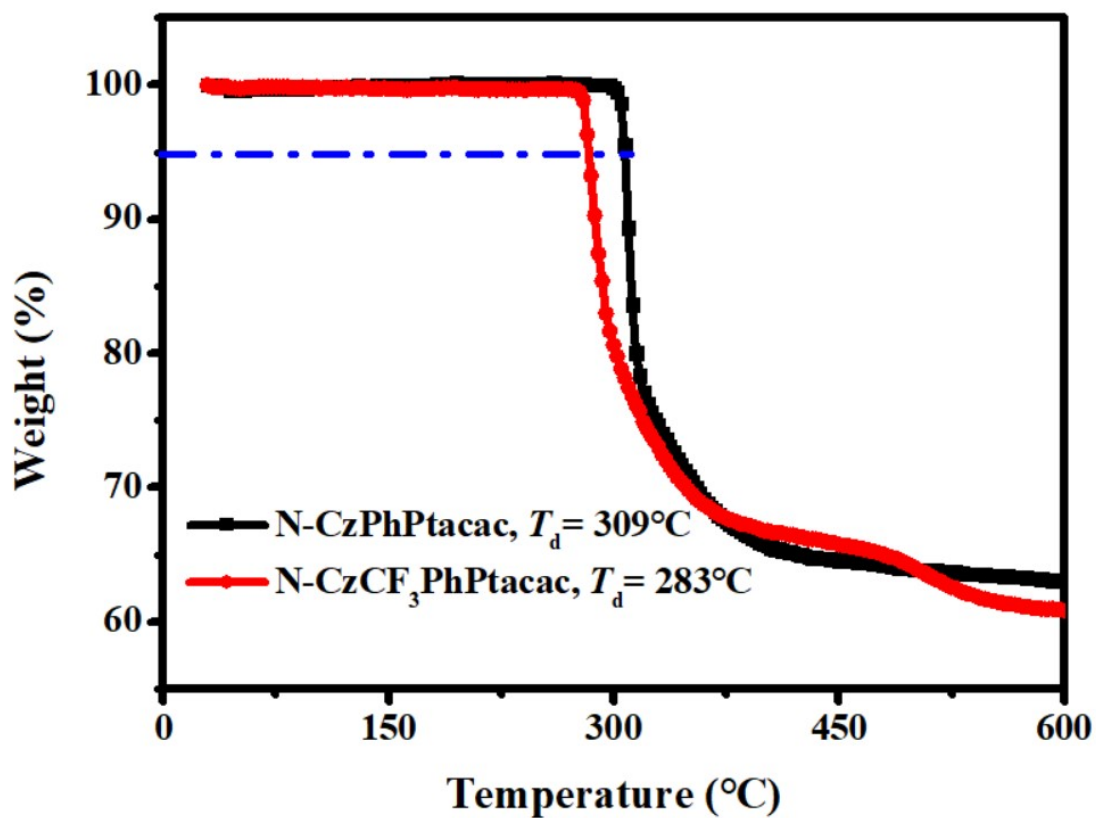


Figure S6. Thermogravimetric analysis (TGA) of two Pt complexes.

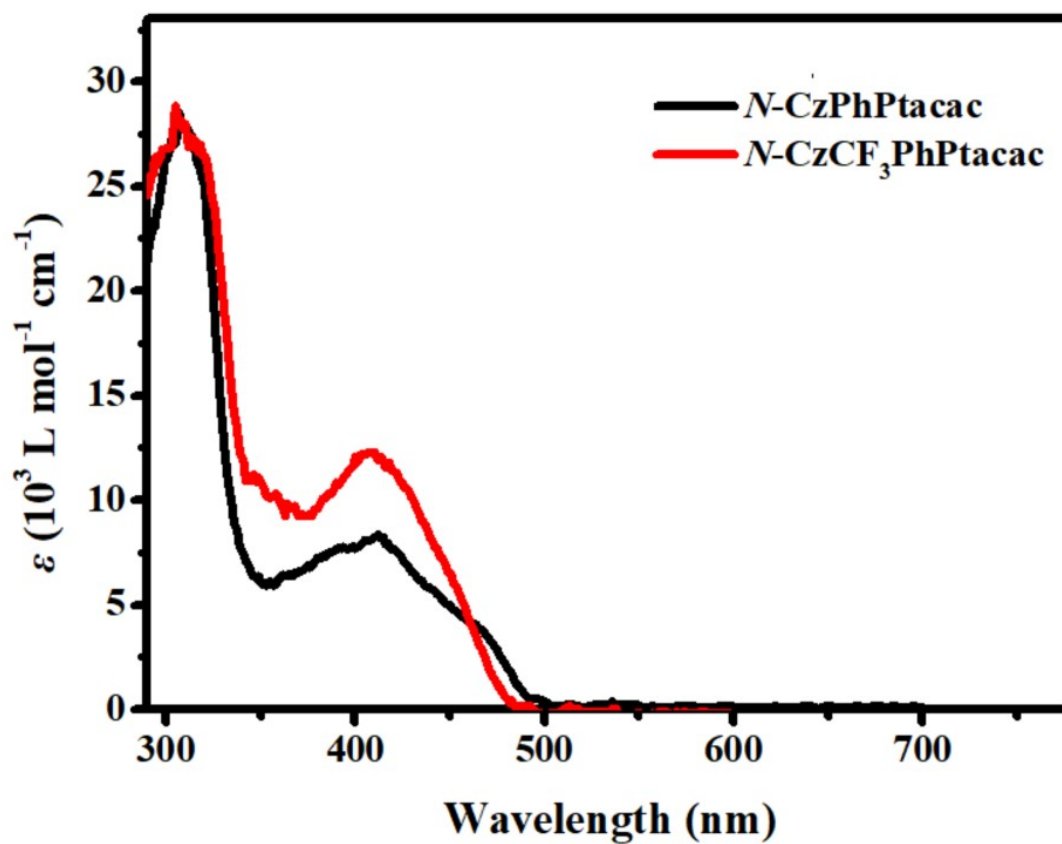


Figure S7. UV-vis absorption spectra at 298K of two Pt scomplexes.

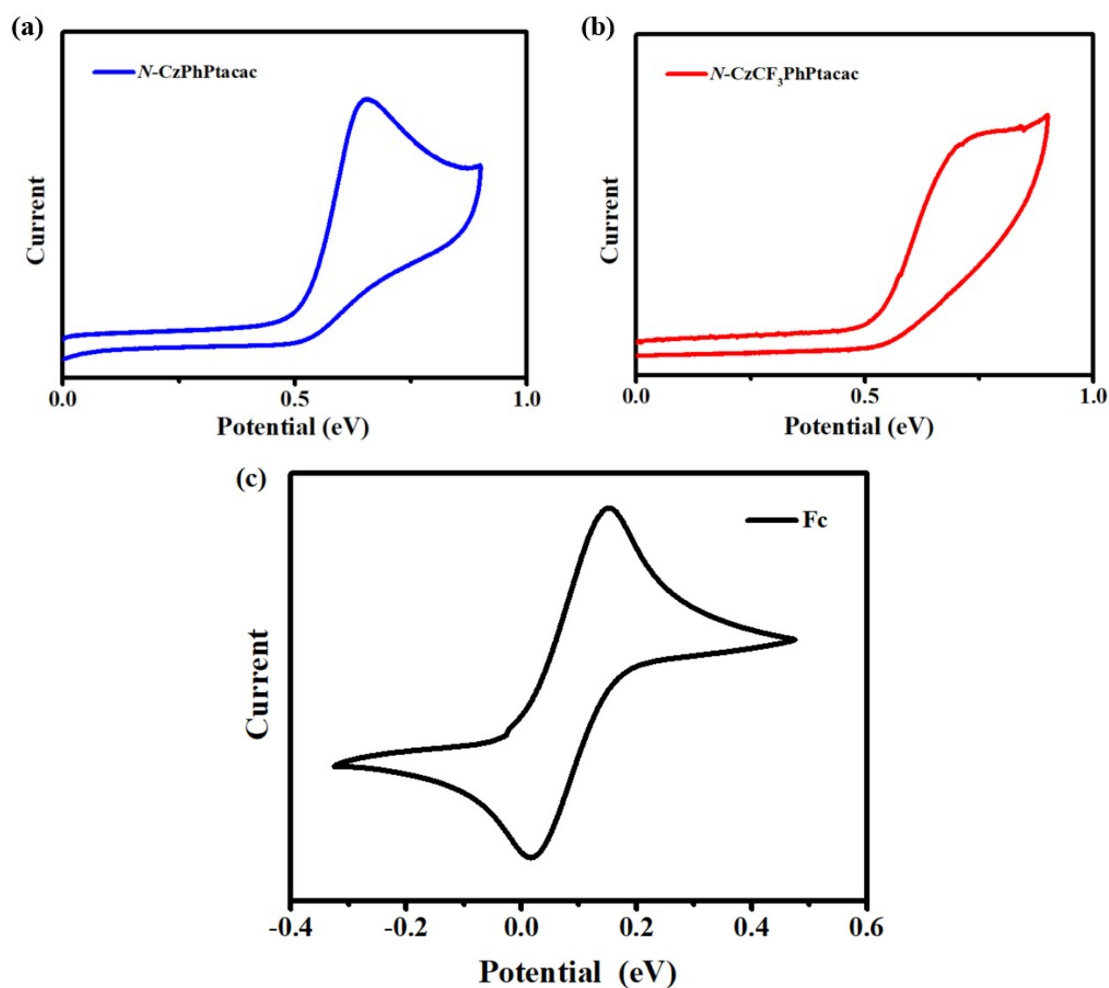


Figure S8. CV curves of (a) *N*-CzPhPtacac, (b) *N*-CzCF₃PhPtacac and (c) ferrocene.

Table S1. Electrochemical properties of *N*-CzPhPtacac and *N*-CzCF₃PhPtacac.

	$E_{(\text{Fc}/\text{Fc}^+)}$	$E_{\text{ox,onset}}^{\text{a}}$	$E_{\text{g,opt}}^{\text{b}}$	$E_{\text{HOMO}}^{\text{c}}$	$E_{\text{LUMO}}^{\text{d}}$
	(V)	(V)	(eV)	(eV)	(eV)
<i>N</i> -CzPhPtacac	0.15	0.63	2.52	-5.28	-2.76
<i>N</i> -CzCF ₃ PhPtacac	0.15	0.65	2.50	-5.30	-2.80

^aThe onset of oxidation curve; ^bOptical gap ($1240/\lambda_{\text{onset}}$); ^c $E_{\text{HOMO}} = -[E_{\text{ox}} - E_{(\text{Fc}/\text{Fc}^+)} + 4.8]$ eV; ^d $E_{\text{LUMO}} = (E_{\text{HOMO}} + E_{\text{g,opt}})$.

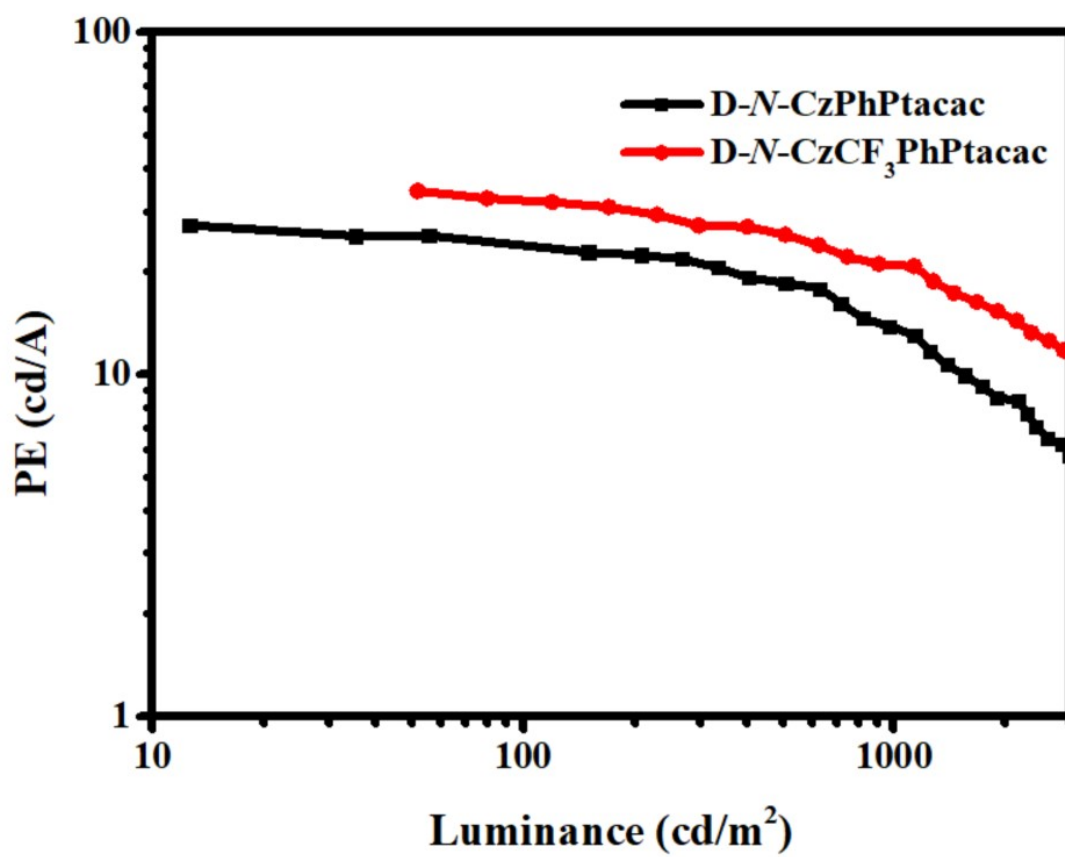


Figure S9. PE-luminance curves of two Pt-based OLEDs.